INTERNATIONAL JOURNAL OF COMPUTERS COMMUNICATIONS & CONTROL
Online ISSN 1841-9844, ISSN-L 1841-9836, Volume: 19, Issue: 2, Month: April, Year: 2024
Article Number: 5732, https://doi.org/10.15837/ijccc.2024.2.5732

CCC Publications

Unveiling the Secrets of Brain Tumors: A Fuzzy C-Means and U-Net Convolution Approach for Enhanced Segmentation

J. Pearline Sheba Grace, P. Ezhilarasi, S. Rajesh Kannan

J. Pearline Sheba Grace, P. Ezhilarasi, S. Rajesh Kannan
Department of Electronics and Communication Engineering
St. Joseph's College of Engineering, OMR, Chennai, India, 600 119
pearlineshebagracej@stjosephs.ac.in, ezhilarasip@stjosephs.ac.in, rajeshkannans@stjosephs.ac.in
*Corresponding author: pearlineshebagracej@stjosephs.ac.in

Abstract

The urge to unveil the secrets of digital visual enhancement has always been a dream for mankind. It has always been an expanding realm of research that has never failed to surprise humanity. In this paper, we have proposed a modified Clustering technique in Fuzzy C-Means named Narrow Fuzzy C-Means Clustering. This clustering method is implemented and fused with U-Net Convolution. The proposed segmentation algorithm uses this unique technique which assists in providing elevated and enhanced outcomes. The suggested approach helps to precisely segment the area of interest from the provided input images. The novel proposal provides an accuracy of 96.5% with a Dice Similarity Co-Efficient (DSC) of 0.94 which tends to determine the exact segmentation of the area of interest with a low false positive rate.

Keywords: Brain Tumor, U-Net Convolution, Fuzzy C-Means Clustering, Anatomical Segmentation, Magnetic Resonance Imaging.

1 Introduction

Tumor image segmentation is based on characteristics including texture, size, density, and so on [1, 2, 3]. An MRI scan's usual display format is black and white to make it easy to distinguish between fluids and tissues. The brain's anatomical structure can be understood, the ROI can be found, and their abnormalities may be examined using MRI [4, 5, 6]. Although the origin of these tumors is unknown, they are certain to cause more serious damage than CT and PET. Due to its superior contrast, this is mostly utilized to diagnose problems in soft tissue organs. Finding the brain's blood vessels and understanding its anatomical structure are both aided by MRI [7, 8].

The major advantage of segmenting images [9, 10, 11, 12] is that instead of processing an entire image, we consider only the features of interest in the image. This helps in improving accuracy and thereby providing much better and clear results. Traditional techniques [13, 14, 15, 16, 17] were easy and simple to understand but as the complexity in input images increases, the accuracy in results drops down exorbitantly [18, 19, 20]. These latest methods use machine and deep learning techniques to improve accuracy and precision to a greater extent [21, 22, 23, 24, 25]. These techniques have been proven to work more efficiently than traditional methods. The basic components when it comes to segmenting an image are an encoder, a decoder, and a series of skip connections [26, 27, 28, 29, 30, 31].

The significant methods for image segmentation include threshold, region-based, edge-based, watershed, and cluster-based methods [32, 33]. Threshold-based methods can be further classified into Otsu's threshold and mean shift methods. The intensity value of the pixels concerning a threshold is used in this method to group them. This classifies grayscale images into two based on their relationship with the threshold value T (high intensity and low intensity), thus producing a binary image. The three types of region-based approaches are region-growing region-split, and region-merged [34, 35]. In this, the similarity is characterized based on features like intensity, color, etc. They contain pre-defined rules that ought to be obeyed by every pixel in that particular region. It involves splitting regions based on similar characteristics. This method is preferred over edge-based methods in case of a noisy image. Edge-based segmentation methods are one of the most popularly used segmentation methods. To utilize this method, the edges of the image need to be identified. This helps in facilitating analysis and also in reducing the size of the pixel [36, 37]. There are quite a lot of methods that perform edge-based segmentation that includes the canny method, gradient method, and Laplacian method. Watershed segmentation methods are based on the extraction of foreground and background such that to extract the exact boundaries of the image. It can be used in segmenting complex images in both manual and automatic segmentation as simple thresholding is not sufficient for segmenting them. The Marker-controlled watershed algorithm [13] helps in locating the boundaries of the overlapping objects to enhance the precision of the watershed segmentation. The last yet most commonly used segmentation technique is the clustering-based method. In other words, this can be called pixel-wise segmentation because similar pixels are grouped into clusters. K-means and Fuzzy C-means clustering are two examples of clustering techniques [38]. An unsupervised approach that is used to segment the area of interest is K-means clustering. This can be done by clustering or partitioning similar pixels or unlabeled data into clusters such that it becomes easy to accomplish segmentation of the images provided. Fuzzy C-means clustering is a technique that is used for segmentation in which the entire dataset of images is clustered into n clusters and each of these clusters is grouped based on the similarity of pixels [39, 40]. The main distinction between these two clustering techniques is that, in K-means clustering, the entire dataset is grouped into a single cluster, but in Fuzzy C-means, the dataset is grouped into k clusters, with each cluster's factor determining how strongly the data are related to it [41, 42].

The goal of segmenting brain tumors is to detect and localize the active tumor tissues, necrotic tissues, and edema [43]. There are certain tumors whose borders are fuzzy and are quite hard to distinguish from healthy tissues. To overcome this, we consider more than one modalities such that to provide a contrast that gives a unique feature to each type of tissue.

The following is the rest of this paper. The bibliological survey is displayed in Sec 2. The proposed methodology is presented in Sec 3. Section 4 discusses and displays the results. Finally, Sec 5 displays the main conclusions.

2 Related Works

Throughout the previous decades, the growth in the realm of processing medical images is tremendous. The various findings and related works in medical image segmentation are being studied and discussed.

Lingling Fang and Xin Wang [3] proposed a Multi-input U-Net model based on the aggregation connection and the integrated block. The accuracy of the suggested model is 92%. It eradicates the problem of vanishing gradients that are caused by the deepening of the network. It also solves low-resolution problems which in turn can increase memory efficiency. The aggregation connection combines deep and shallow information from the brain with formidable spatial and geometric relationships. Paturi Jyothsna et al [4] presented a more advanced version of a U-Net model based on a neural network that is fully convolutional for segmenting tumors of the brain. When compared to manual segmentation, they have proven to deliver better and more efficient segmentation. As they use a Fully Convolutional Network (FCN), it guides the correspondence of input and output images at the level of pixels. The DSC of the proposed algorithm is said to be 0.79.

Jason Walsh et al [14] presented a lightweight U-Net architecture. The suggested model can be trained without the need for extensive datasets. The proposed algorithm was implemented with the help of TensorFlow. It is proven to have performed better when compared to the benchmark algorithms that were considered for the comparative analysis. The accuracy of the suggested algorithm is found to be 99.2%. Pallavi Asthana et al [16] attempted an algorithm for the semantic segmentation of brain tumors which is based on the U-Net algorithm. For survival prediction of patients, they have introduced a regression model. Regression model weights are based on the ubiquitous learning model. The trained model yields a DSC of 0.91 and the regression model attains a precision of 64.2% on the survival prediction of patients. The recommended method is found to be superior and gives robust segmentation.

Numerous studies in recent years have highlighted trends and challenges in the precise segmentation of tumors based on MRI images [29, 38, 42]. Many segmentation algorithms are based on an advanced version of the U-net model [3, 4, 14, 16], fully automated Convolutional Neural Networks (CNN) [11, 40], modified BU-net [30], Marker-controlled Watershed segmentation [13] and Z-Net [12].

3 Methodology

3.1 Introduction

In this article, a unique method by combining Fuzzy C-means and CNN is proposed to increase the accuracy along with other parametric measures. This algorithm is used to detect the features and region of interest (ROI) and helps in aiding clinicians in expert and precise results. The proposed work uses the images from the pre-described labeled dataset for further study. The dataset contains MR images of about 55 patients which includes both normal and abnormal patients. Figure 1 represents the workflow of the proposed work. The diagrammatic representation helps in understanding how the proposed algorithm works. This helps in understanding the algorithm's overall efficiency.

3.2 Pre-Processing by Adaptive non-local median Filtering

To pre-process and restore the input image, we have introduced a new adaptive non-local median filter (ANMF) which can be used as a non-linear digital filtering operation that aids in removing salt and pepper noise. AMFs replace every pixel with the median pixel value within the neighborhood that surrounds the pixel whereas, in ALMF each pixel is replaced with a weighted value of similar pixels in the image. AMFs are considered over other filters because of their advantages. This includes their robustness to impulsive noise than mean filters as they replace every pixel with the surrounding neighborhood which makes them less sensitive to outliers. Next is their ability to preserve the edges of the images. Next, the ability of this filter to restore images that have non-uniform noise distributions makes this an ideal choice for filtering and restoring images. The last yet final characteristic of having simple implementation and low computational cost makes it quite a catch in the process of restoring and filtering images.

Though there are many advantages to considering AMFs, it is time-consuming as we need to replace every pixel with its median pixel in its neighborhood. Thus, we have proposed an Adaptive Non-Local Median Filter that helps by weight factor as the noise decision criteria instead of searching every pixel in each window which in turn will reduce complexity and processing time. The weight factor can be calculated with the help of the Manhattan distance. Let $I(x, y)$ imply the input image where (x, y) denotes the pixel coordinates. The median filter with a window size of $N \times N$ can be defined as,

$$I_{filtered}(x, y) = median(w(x, y, p, q) * I(x + i, y + j)) \tag{1}$$

where $I_{filtered}(x, y)$ - filtered output value at coordinates (x, y)

$I(x + i, y + j)$ - intensity values of all pixels within the specified window centered at (x, y)

$w(x, y, p, q)$ - similarity measure between reference patch centered at (x, y) and the patches at location (p, q) within the search window Equation (1) represents the filtered output value using the

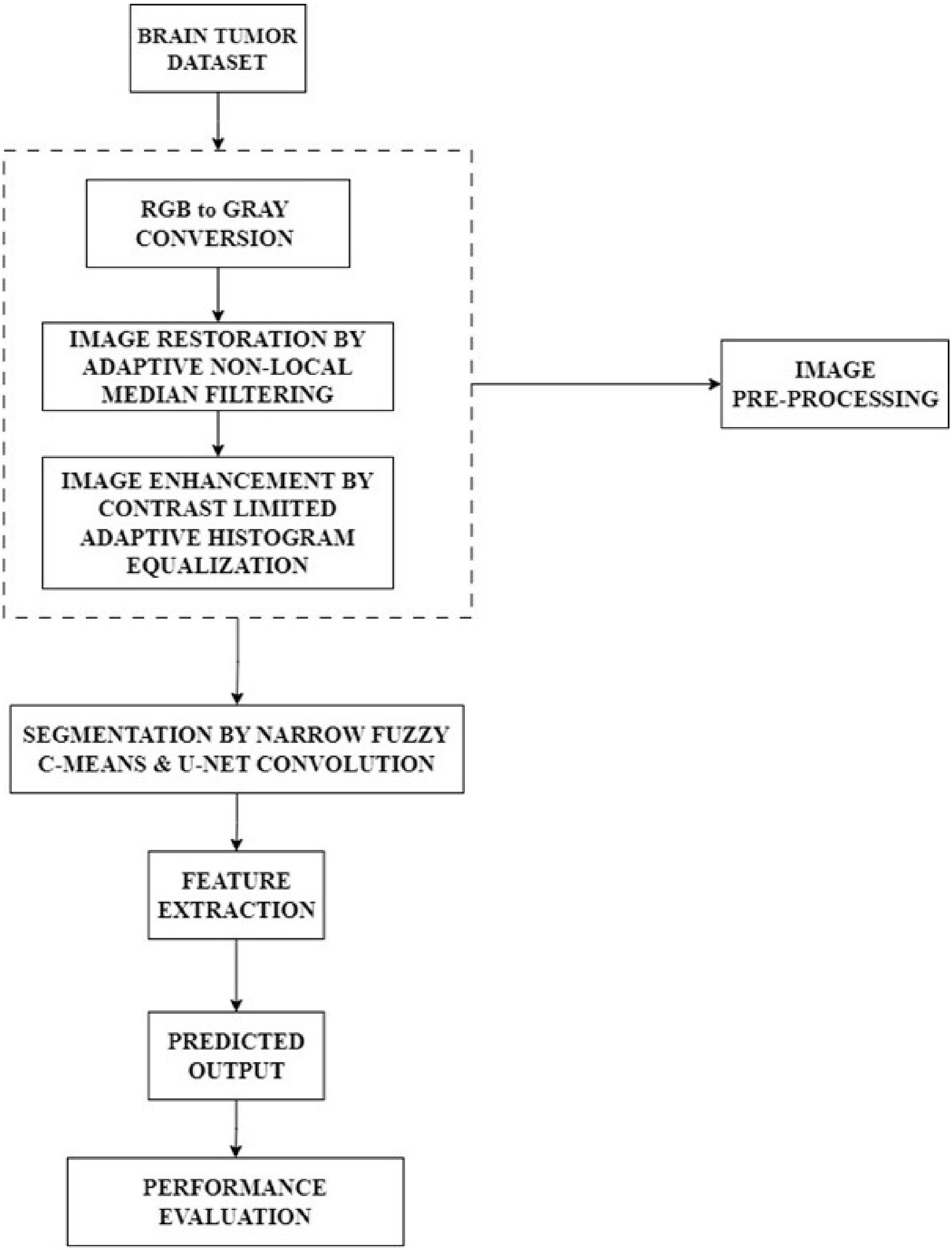

Figure 1: Workflow of the proposed algorithm

Adaptive Non-Local Median Filter whereas Eq (2) denotes the formula for calculating Manhattan distance which is proven to be more effective. The ideal weight factor should be selected based on specific noise characteristics. The ideal weight factor for denoising Gaussian noise and salt and pepper noise has been selected as 0.3 and 0.8 respectively based on experimentation. The weights can be calculated with the help of Manhattan Distance where the sum of absolute differences provides the total distance between two points. It can be represented by,

$$d = |x_2 - x_1| + |y_2 - y_1| \tag{2}$$

where x & y are the variables. After pre-processing, the images are enhanced with the help of Contrast Limited Adaptive Histogram Equalization (CLAHE).

3.3 Segmentation by Narrow Fuzzy C-Means Clustering with U-Net Convolution

Once all these images are pre-processed and enhanced, the next step is to apply the segmentation algorithm. In this article, we have presented a fusion technique that combines a clustering algorithm with a segmentation algorithm. This algorithm aids in improving the accuracy and other parametric measures to a notable level. The proposed fusion method combines Fuzzy C-Means (FCM) clustering with U-Net, a neural network segmentation algorithm.

3.3.1 Narrow Fuzzy C-Means Clustering

FCM is an iterative clustering algorithm, which helps in segregating pixels based on their similarities. Contrary to conventional approaches, FCM enables a pixel to belong to many clusters with varying degrees of membership, making it possible to separate pixels that are spread across multiple clusters. Contrary to conventional approaches, FCM enables a pixel to belong to many clusters with varying degrees of membership, making it possible to separate pixels that are spread across multiple clusters. This process of FCM helps in minimizing the cost function.

In our proposed work, we have introduced a novel method known as a Narrow FCM which helps further narrow down the process of clustering. This method of clustering assists in reducing the time required for clustering. Generally, in FCM we find objective and fuzzy membership functions along with centroid calculation. But in the case of Narrow-FCM, we consider boundary regions along with lower and higher approximation regions. This consideration of regions helps in reducing the complexity and time consumption which are the disadvantages of the process of traditional clustering. This also helps in dealing with incompleteness and uncertainty in each class that has been defined. In addition to this fuzzy membership, functions deal efficiently with overlapping partitions.

Consider $A(\alpha_i)$ as the pessimistic estimate of cluster i, $\bar{A}(\alpha_i)$ as the optimistic estimate of cluster i, and $B(\alpha_i)$ as the peripheral region of cluster i. The peripheral region of cluster i can be represented by,

$$B(\alpha_i) = \{\bar{A}(\alpha_i)/A(\alpha_i)\} \tag{3}$$

Where α_i - representation of cluster i.

The above-given Eq (3) denotes the formula for calculating the peripheral region of the given cluster. Consider X_j as the elements present in each cluster. Some conditions need to be satisfied, these include,

1. If $X_j \in A(\alpha_i)$, then $X_j \notin B(\alpha_i) \forall j$
2. If $X_j \in B(\alpha_k) \forall k$, where $k \neq i$

where α_i & α_k are the representation of clusters k & i.

The conditions that are to be satisfied depend on the threshold value δ. It is characterized as the average difference between the two highest membership functions taking into account all dataset items. The threshold value can be represented as,

$$\delta = \frac{1}{n} \sum (\mu_{ij} - \mu_{kj}) \tag{4}$$

Where n - number of elements

μ_{ij} & μ_{kj} - highest & second highest membership of an element X_j to the cluster α_i & α_k

Equation (4) symbolizes the mathematical representation of the threshold value. The higher the value of the threshold, the better the clustering results. Because NFCM can divide the given dataset into pessimistic estimates and boundary portions of the cluster, the value of δ has a major influence on the overall efficiency of Narrow-FCM. For NFCM, we need to calculate the objective function and centroid calculation. The objective function can be represented by

$$J_{NF} = \begin{cases} (w_l \times P) + (w_b \times Q), & \text{if } A(\beta_i) \notin \emptyset, B(\beta_i) \notin \emptyset \\ P, & \text{if } A(\beta_i) \notin \emptyset, B(\beta_i) \in \emptyset \\ Q, & \text{if } A(\beta_i) \in \emptyset, B(\beta_i) \notin \emptyset \end{cases} \tag{5}$$

Where $P = \sum_{i=1}^{c} \sum_{X_j \in A(\beta_i)} \|X_j - V_i\|^2$

$Q = \sum_{i=1}^{c} \sum_{X_j \in B(\beta_i)} (\mu_{ij})^{m_1} \|X_j - V_i\|^2$

w_l - parameter of lower approximation

w_b - parameter of a boundary region

The centroid calculation for NFCM can be given by,

$$V_i = \begin{cases} (w_l \times X) + (w_b \times Y), & \text{if } A(\beta_i) \notin \emptyset, B(\beta_i) \notin \emptyset \\ X, & \text{if } A(\beta_i) \notin \emptyset, B(\beta_i) \in \emptyset \\ Y, & \text{if } A(\beta_i) \in \emptyset, B(\beta_i) \notin \emptyset \end{cases} \tag{6}$$

Where, $X = \frac{1}{|A(\beta_i)|} \sum_{X_j \in A(\beta_i)} X_j$

$Y = \frac{1}{n_i} \sum_{X_j \in B(\beta_i)} (\mu_{ij})^{m_1} X_j$

$n_i = \sum_{X_j \in B(\beta_i)} (\mu_{ij})^{m_1}$

m_1-fuzzifier $(0 \le m_1 < \infty)$

The centroids of the clusters depend on these parameters

$$w_l + w_b = 1, 0 < w_b < w_l < 1 \tag{7}$$

$$w_b = (1 - w_l) \tag{8}$$

If $w_l = 1$ & $w_b = 0$, then the proposed FCM's performance is somewhat diminished because the corresponding cluster can't handle the elements of the boundary region, and thus the centroid will be stuck. Consider X_j as the lower approximation in a cluster α_i, then w_l is significantly larger when compared to w_b for the elements that belong in the boundary region of the cluster α_i. Equations (5) & (6) signify the objective function and centroid calculation for Narrow Fuzzy C-Means Clustering whereas Eq (7) & (8) denote the conditions on which the centroids of the clusters depend. Once clustering is performed using the proposed Narrow-FCM, the clustered label data is converted into a binary mask which will be provided as input to the architectural U-Net model. The clustered data is represented by a unique binary value which means the cluster is denoted by 1 and 0 for everything else. The distinct binary mask is provided to the U-net structure as input.

3.3.2 U-Net convolution architecture

U-net architecture is a CNN architecture that helps in localizing and distinguishing the area of abnormality. Both input and output images share the same pixel size. This is highly used in medical images as it is highly necessary to not only distinguish the abnormality but also to localize the tumor region. This architecture is symmetric and includes two different paths. They are the contracting path and the expansive path. The contracting path resembles the traditional convolutional neural network architecture, whereas the expansive path resembles the transposed 2D convolutional layers. The encoder or contracting path down-samples the input data and extracts the features at different layers and then the decoder or expansive path up-samples the path and improves segmentation. In this, we combine the previous layers such that to get a more precise prediction which will in turn improve accuracy. In our proposed method, we use MRI data as input because it is one of the most sensitive imaging modalities for understanding the human anatomy and vertebral column of each individual. It functions by stimulating hydrogen protons present in the tissues of the human anatomy. These tissues when stimulated produce an electromagnetic signal that is given to the MRI machine. These images are sensed based on their intensity values and are then transformed into grayscale MRI scans. In MRI, low and high-intensity signals are used to represent the brain's anatomical structure and appearance. Bones are generally low in intensity and are represented as the darkest regions of the scan. These representations use black, white, and gray colors to understand and study the input MRI images. Thus, radiological contrast helps in understanding the visual perception that differentiates between the inspected anatomical structure and the tissue surrounding it. In our proposed method, we have used N-FCM to provide a mask image that can be used as an input to the U-Net architecture. The encoding path or up-sampling helps in understanding what is present in the image whereas the decoding path or down-sampling helps in recovering where the exact information is present in the image. Thus, the encoding and decoding paths together make up the entire architectural model.

The contracting path replicates the convolutional neural architecture of the network that sub-samples the provided image. Two 3×3 unpadded convolutions and a rectified linear activation unit (ReLU), which is applied after each down-sampling, make up this algorithm. After that, a 2×2 max-pooling procedure follows. Each stage of the down-sampling procedure increases the number of feature channels. Each stage in the expanded path includes a 2×2 up-convolution, reducing the number of feature channels. Each ReLU is followed by two 3×3 convolutions, and it is concatenated with the proportionately smaller feature maps from the encoding path. Each convolution causes a loss of pixels that are present in the given image's borders, necessitating the use of snipping. The 64-component feature is then separated using a 1×1 convolution in the last layer. In this network architecture, there are 23 layers in the convolutional layer. The U-Net convolution algorithm proceeds as follows:

1. Preprocessing the given image datasets.

2. This is the contracting path, where the size of the image gradually shrinks from $128 \times 128 \times 2$ to $8 \times 8 \times 512$ as the intensity of the image gradually increases with convolutions that are standard and a max-pooling 2×2 unit in each level.

3. The contracting path consists of nine convolutions with a standard kernel size of 3×3 and 'ReLU' is the activation function which is proceeded by a max pooling layer with a pool size of 2×2

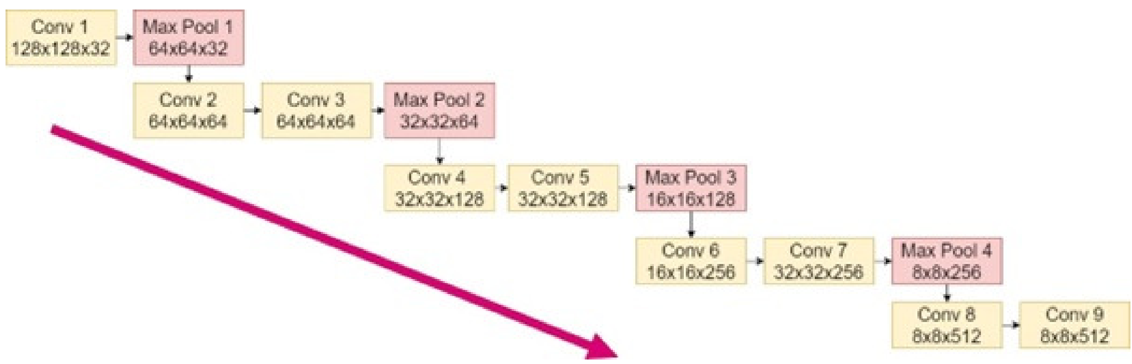

Figure 2: Contracting Path

4. Then, comes the expansive path that includes transposed convolutions accompanied by standard

convolutions which progressively augment the image size while contracting the intensity or depth of the image from $8 \times 8 \times 512$ to $128 \times 128 \times 2$.

5. The expansive path consists of standard convolutions with a kernel size of 3×3. Up-sampling is performed with a standard kernel size of 2×2 and an activation function of ReLU. Figure 2 showcases the flow of the contracting path in U-net Convolution.

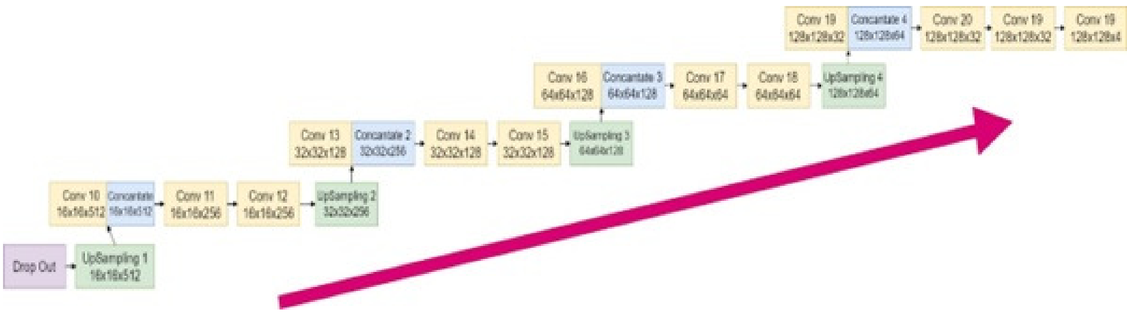

Figure 3:

6. The encoder-decoder are connected with the help of skip-connections and are then concatenated with the layers in the decoder. Thus, the U-net effectuates an image in the expansive path using the fine-grained details that have been extracted from the contracting path. Figure 3 depicts the flow of the expansive path in U-net Convolution.

In the final layer, the activation function used is 'Softmax'. Figure 4 below denotes the proposed U-Net convolution architecture. The proposed architecture is a U-net architecture that is fused with Narrow Fuzzy C-Means Clustering Algorithm. This helps in segmenting the ROI precisely.

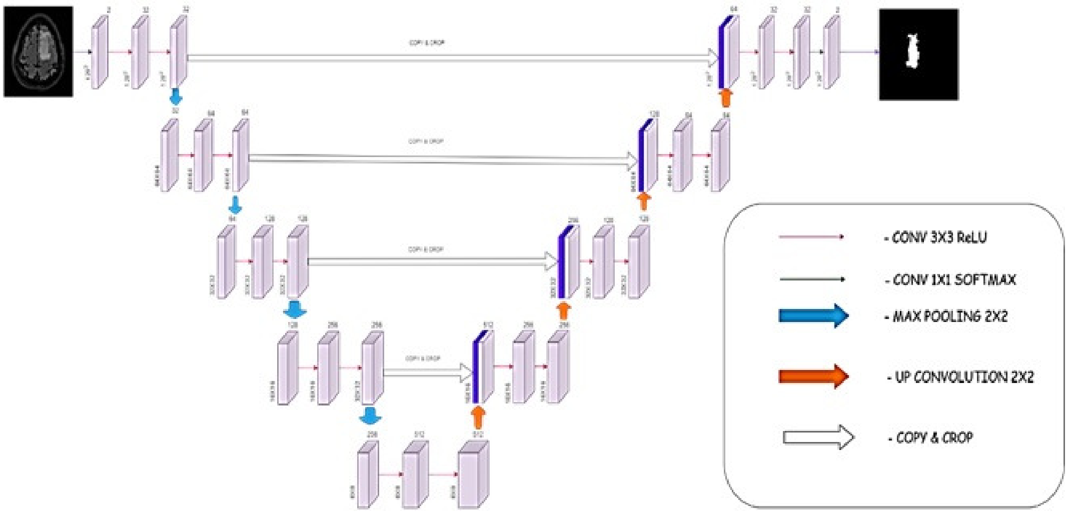

Figure 4: Proposed U-Net Architecture

The u-net architecture uses a network that is fully convolutional for semantic segmentation. The major purpose of using semantic segmentation is to assign a class to every pixel that will symbolize something in the given input image. This type of assigning classes to pixels is referred to as dense prediction since we predict each pixel in the input image such that to improve the parametric features.

3.4 Evaluation Metrics

The parameters that have been used for evaluating the proposed algorithm include Precision, Accuracy, Sensitivity, Specificity, and Dice Coefficient. Each of these parameters is represented with the assistance of the below-given mathematical expression,

$$\text{Accuracy} = \frac{(TP + TN)}{(TP + FP + FN + TN)} \tag{9}$$

$$\text{Precision} = \frac{(TP)}{(TP + FP)} \tag{10}$$

$$\text{Specificity} = \frac{(TN)}{(TN + FP)} \tag{11}$$

$$\text{Sensitivity} = \frac{(TP)}{(TP + FN)} \tag{12}$$

$$\text{Dice Co-efficient} = \frac{2 * TP}{FN + FP + (2 * TP)} \tag{13}$$

Equations (9) - (13) denote the formulae that are used for evaluating parametric measures like accuracy, precision, specificity, sensitivity, and dice co-efficient respectively. Accuracy is the relation between the measured and target value which is crucial for making choices in diagnosis whereas precision refers to the level of consistency when the same algorithm is repeated under similar conditions. Precision serves as a benchmark for evaluating and maintaining the quality of an algorithm. Specificity refers to the processes of identifying the non-target regions accurately whereas sensitivity refers to the processes of identifying the target or true positive instances accurately. When compared to existing algorithms, the suggested method that combines u-net architecture and fuzzy-based C-means yields significantly better results. In clinical applications, higher parametric measures indicate better segmentation that indicates more reliable and relevant results.

4 Results and Discussions

The proposed algorithm includes segmentation and clustering with image acquisition, image pre-processing, and image enhancement. Image acquisition includes the conversion of an RGB image into a gray-scale image which is done by calculating the intensity and size of the image. This is depicted in Fig 5(a).

The pre-processing techniques consist of an Adaptive Non-Local Median Filter which assists in removing salt and pepper noise which is one of the major issues when it comes to denoising in MR images. The image that is filtered using ANMF is depicted in Fig 5(b). This technique is quite innovative since it can be used for both salt and pepper noise as well as Gaussian noise. The noise content in the image is showcased in Fig 5(c). The above-mentioned technique for noise removal is unique since it uses the weight factor as the noise decision criteria, thus reducing the complexity and time consumption.

Image enhancement is a necessary procedure since removing noise from the images could result in some loss of the necessary image. In this paper, we have used CLAHE. It helps in improving the contrast of the provided image. Image enhancement using CLAHE is portrayed in Fig 5(d). The below-given figure denotes the stages of processing an input image before obtaining the segmented result. Figure 5(a) shows the input image, whereas Fig 5(b-f) denotes image filtering using ANMF, noise content in the filtered image, image enhancement using CLAHE, image clustering using Narrow-FCM, and Segmented output image respectively. This helps in providing a much better insight into understanding what happens in each stage of the algorithm.

In this paper, we have considered grade II and III tumors. These grade II tumors are referred to as low-grade tumors (LGG) whereas grade III are known as high-grade tumors (HGG). Grade II can

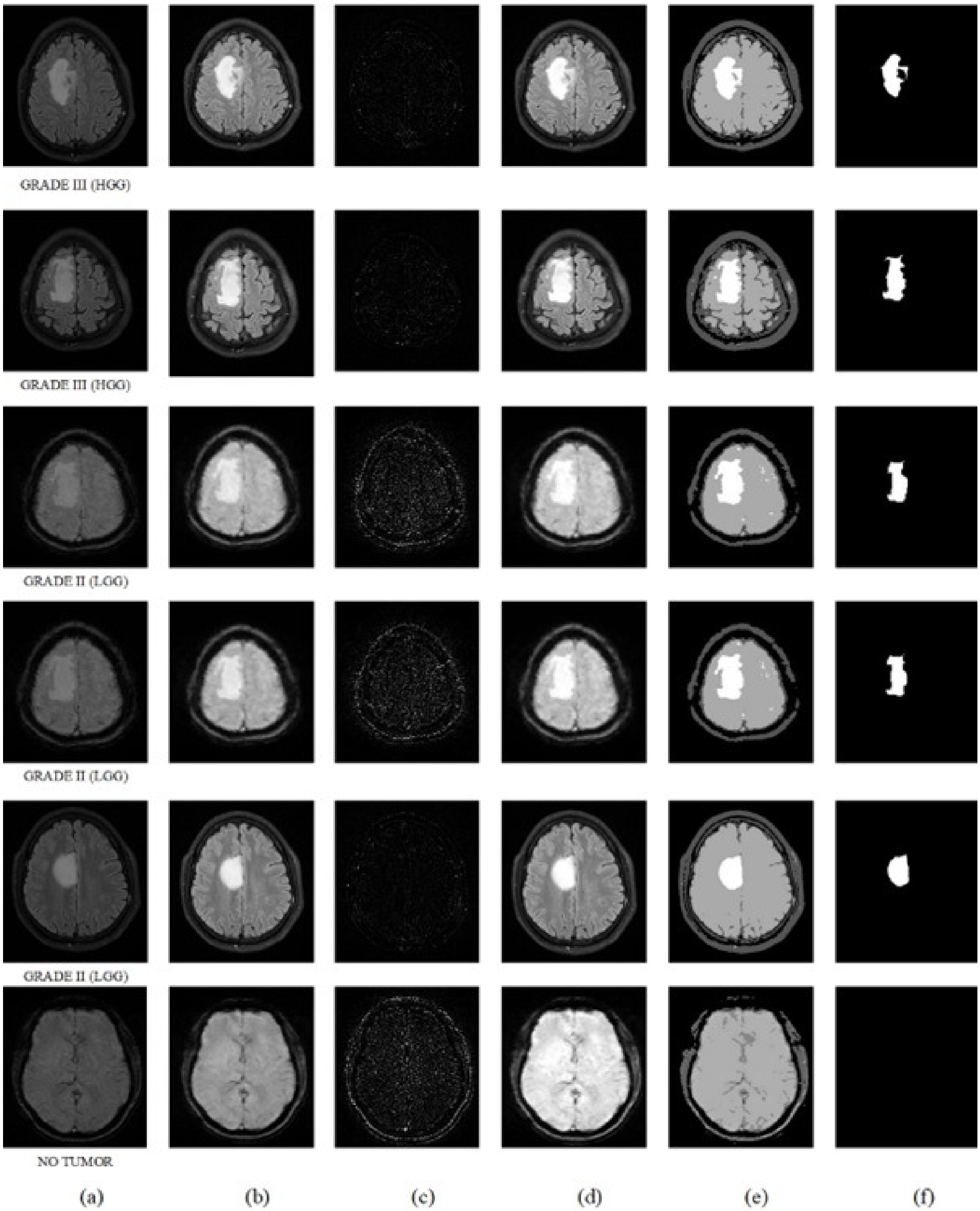

Figure 5: (a) Input Image, (b) Image Filtering using Adaptive Non-Local Median Filter, (c) Noise Content in the Filtered Image, (d) Image Enhancement using CLAHE, (e) Image Clustering using Narrow FCM and (f) Segmented Output Image

Table 1: Comparison of parametric measures

Methods	Accuracy (%)	Precision (%)	Specificity (%)	Sensitivity (%)	Dice Similarity Co-efficient (DSC)
U-Net Convolution with Narrow Fuzzy C-Means Clustering	96.5	92.8	86.34	90.2	0.94
Z-Net (Mohammad Ashraf Ottom et al, 2022) [12]	95.7	94.92	87.45	96.32	0.91
GoogLeNet (Sunita M Kulkarni, 2020) [31]	93.89	93.75	89.23	97.12	0.92
Multi-Input U-net Model (Lingling Fang & Xin Wang, 2020) [3]	92	90.24	89.2	97	0.83
Fuzzy C-Means and Genetic Algorithm (Nitesh Bhaskarrao Bahadure et al, 2018) [38]	92.03	91.62	91.42	92.36	0.93
Convolutional Neural Networks (Sergio Pereira et al, 2016) [41]	94.63	93.34	92.89	91.6	0.88

eventually develop into their higher-grade versions. Grade III tumors are more assertive and invasive. HGG tends to be aggressive and is hard to remove by surgical means since it evades the nearby tissue region surrounding the tumor region.

The proposed algorithm cannot be implemented directly on RGB images since they are hard to work on. To avoid this, we convert them to gray-scale images, which will help to easily segment MR images. This algorithm facilitates analysis and quickly delivers an accurate conclusion. The suggested algorithm combines narrow Fuzzy C-Means Clustering, an innovative technique, and a U-Net algorithm.

Clustering pixels with similar features are grouped, so that it becomes easy for us to differentiate ROI from the robust region of the brain. The image that is clustered based on Narrow FCM Clustering is exhibited in Fig 5(e).

The suggested method's accuracy is rather high due to its ability to separate the tumor region from the input images. It aids in providing an output that is true to the ground truth. The segmented output using the proposed method is depicted in Fig 5(f). Higher accuracy is crucial for making a correct diagnosis based on imaging. We know that accuracy serves as a benchmark for measuring the effectiveness of the image processing algorithm. Hence, an accuracy of 96.5% shows that the proposed algorithm is effective for segmenting tumor regions from the given set of input images.

The figure above denotes the proposed algorithm's comparative analysis with various techniques. Figure 6(a) shows the analysis of the Accuracy compared with other methods whereas Fig 6(b-e) shows the analysis of other parametric measures such as Precision, Specificity, Sensitivity, and Dice Similarity Co-Efficient respectively. The pictographic representation of the comparative analysis helps in a clear understanding of the importance of the proposed algorithm.

The accuracy and specificity values tend to perform better when compared to other techniques. This study helps understand the relationship between the parametric measures that have been considered. The relationship between accuracy and precision is that accuracy focuses on the faithfulness of the segmented output to the anatomical image whereas precision focuses on the consistency of observations by using the proposed algorithm.

Algorithms with higher accuracy make them more suitable for critical applications whereas the ones with higher precision make them more reliable for specific applications. Table 1 showcases the comparative analysis of parametric measures with the proposed algorithm. Precision directly affects the accuracy of an algorithm. Specificity refers to the algorithm's capability to correctly classify

Figure 6: Comparative Analysis of (a) Accuracy, (b) Precision, (c) Specificity, (d) Sensitivity, and, (e) DSC

regions the non-target regions in an image whereas sensitivity refers to the capability of an algorithm to correctly classify the target regions in the given image. Algorithms with higher specificity make them more reliable and indicate their ability to detect non-target regions whereas the ones with higher specificity make them more suitable and show their ability to identify target regions correctly.

The primary goal of employing parametric measurements like sensitivity and specificity is to eliminate false positives and negatives, which directly impact the proposed algorithm's overall performance. The spatial gap between ground truth and segmented output in the image segmentation stream is referred to as DSC. A complete overlap between the target image and the segmented output tends to indicate that the segmented output is the same as that of the ground truth.

The proposed algorithm provides an accuracy of 96.5% which is higher as the ability to focus on the faithfulness of the segmented output to the anatomical image is greater when compared to similar techniques. The precision of the proposed method is said to be about 92.8%. We know that precision concentrates on the consistency of the proposed algorithm in producing observations. In our proposed algorithm, the consistency of observations was not up to the mark and requires improvement. Other parameters like specificity and sensitivity are taken into consideration. The process of identifying false positives and false negatives plays an important role since they directly affect accuracy and precision.

The proposed method of fusing FCM clustering with the U-net algorithm provides better and enhanced outcomes with an accuracy of about 96.5%, a precision of 92.8%, a specificity of 86.34%, a sensitivity of 90.2% and a disc similarity co-efficient of 0.94 respectively. The u-net convolution is generally performed to segment images fast and precisely. But, performing this convolution for large datasets can cause havoc since it consumes a huge amount of time. So to avoid this, we have proposed an algorithm that will help reduce the processing time and provide precise results.

5 Conclusion and Future Work

Segmentation is performed on images to obtain an output with a desired level of detail in the segmented output. The area of research has a propitious future since there is always space for improvement in the parametric measures such as precision, accuracy, specificity, and sensitivity. The Proposed Method uses U-Net Convolution fused with Narrow-FCM Clustering which is proven to be much more efficient and effective when compared to authentic and original segmentation by using Clustering methodology. The specifications that are considered show a drastic and exponential increase, thus providing a much superior image quality of the segmented output. The accuracy of U-Net Convolution fused with the Narrow-FCM Clustering Algorithm is said to be 96.5% and the Dice Similarity Co-Efficient (DSC) is about 0.94, thus proving that the segmented output is much better in clarity. The segmented output provides better clarity and faithfulness to the ground truth making it trustable. Thus, we have proved that the above-described algorithm provided a much more efficient result when compared to other segmentation techniques. Even though our suggested approach is more accurate than the prior methods, several parametric measures still need to be improved. Parametric measures like precision and sensitivity need to be given extra attention as identifying false negatives and positives is more crucial when segmenting brain tumors. Since these parameters determine the final decision before opting for tumor removal through surgery. Hence, improvement needs to be done in certain parametric measures such as precision and sensitivity.

Conflicts of Interest

No potential conflict of interest was reported by the author(s).

Authors Contributions

Ezhilarasi and Rajeshkannan are the co-authors of this paper. Ezhilarasi contributed in the literature survey. Rajeshkannan implemented and evaluated the image segmentation. Pearline Sheba Grace contributed to the study and draft of the manuscript. All authors contributed to data preparation and revision of the manuscript for exclusive content.

References

[1] Soomro, T.A.; Zheng, L., Afifi, A.J., Ali, A., Soomro, S., Yin, M., Gao, J. (2023). Image Segmentation for MR Brain Tumor Detection Using Machine Learning: A Review, *IEEE Rev Biomed Eng.* 70–90, 2023.

[2] Ramya, D.; Lakshmi, C. (2023). Brain Tumor Segmentation using MRI Images by Optimized U-Net, *In 2023 International Conference on Networking and Communications (ICNWC)*, 1–6, IEEE, 2023).

[3] Lingling Fang; Xin Wang (2023). Multi-input U-net model based on the integrated block and the aggregation connection for MRI brain tumor segmentation,*Biomedical Signal Processing and Control*, 79(1), 104027, 2023, ISSN: 1746-8094, https://doi.org/10.1016/j.bspc.2022.104027.

[4] Jyothsna, P. et al. (2023). Brain Tumor Segmentation Using U-Net,. In *Ogudo, K.A., Saha, S.K., Bhattacharyya, D. (eds) Smart Technologies in Data Science and Communication*, Lecture Notes in Networks and Systems, Springer, Singapore, 558, 2023. https://doi.org/10.1007/978-981-19-6880-8_16

[5] Allah, A.M.G.; Sarhan, A.M., Elshennawy, N.M. (2023). Edge U-Net: Brain tumor segmentation using MRI based on deep U-Net model with boundary information, *Expert Systems with Applications*, 213, 118833, 2023.

[6] Kumar, G.M.; Parthasarathy, E. (2023). Development of an enhanced U-Net model for brain tumor segmentation with optimized architecture, *Biomedical Signal Processing and Control*, 81, 104427, 2023.

[7] Sangui, S.; Iqbal, T., Chandra, P.C., Ghosh, S.K., Ghosh, A. (2023). 3D MRI Segmentation using U-Net Architecture for the detection of Brain Tumor, *Procedia Computer Science*, 218, 542–553, 2023.

[8] Raza, R.; Bajwa, U.I., Mehmood, Y., Anwar, M.W., Jamal, M.H. (2023). dRes$U$-Net: 3D deep residual U-Net-based brain tumor segmentation from multimodal MRI, *Biomedical Signal Processing and Control*, 79, 103861, 2023.

[9] Poonguzhali, R.; Ahmad, S., Sivasankar, P.T., Anantha Babu, S., Joshi, P., Joshi, G.P., Kim, S.W. (2023). Automated brain tumor diagnosis using deep residual u-net segmentation model, *Computers, Materials & Continua*, 74(1), 2179–2194, 2023.

[10] Shiny, K.V. (2023). Brain tumor segmentation and classification using optimized U-Net, *The Imaging Science Journal*, 1–16, 2023.

[11] Swathi, P.; Narayana Ramakrishna, M., Vilasini, K., Sai Hemanth, M., Nirmal Sumanth, J. (2022). 3D U-Net for Brain Tumor Detection and Segmentation, *International Journal of Scientific Research in Science and Technology (IJSRST)*, Print ISSN: 2395-6011, Online ISSN: 2395-602X, 9(3), 415–421, 2022.

[12] Ottom, M.A.; Rahman, H.A., Dinov, I.D. (2022). Znet: Deep Learning Approach for 2D MRI Brain Tumor Segmentation, *IEEE Journal of Translational Engineering in Health and Medicine*, 10, 2022, doi: 10.1109/JTEHM.2022.3176737. PMID: 35774412; PMCID: PMC9236306.

[13] Grace, J.P.S.; Ezhilarasi, P. (2022). Enhanced Marker-Controlled Watershed Segmentation Algorithm for Brain Tumor Segmentation. In: *Mukhopadhyay, S., Sarkar, S., Dutta, P., Mandal, J.K., Roy, S. (eds) Computational Intelligence in Communications and Business Analytics (CICBA 2022), Communications in Computer and Information Science*, Springer, Cham, 1579, 2022. https://doi.org/10.1007/978-3-031-10766-5_12.

[14] Jason Walsh; Alice Othmani, Mayank Jain, Soumyabrata Dev. (2022). Using U-Net network for efficient brain tumor segmentation in MRI images, *Healthcare Analytics*, 2, 100098, 2022, ISSN: 2772-4425, https://doi.org/10.1016/j.health.2022.100098.

[15] Nasim, M.A.; Munem, A.A., Islam, M., Palash, M.A., Haque, M.M., Shah, F.M. (2022). Brain Tumor Segmentation using Enhanced U-Net Model with Empirical Analysis, 2022, ArXiv. /abs/2210.13336.

[16] Asthana, P.; Hanmandlu, M., Vashisth, S. (2022). Brain tumor detection and patient survival prediction using U-Net and regression model, *International Journal of Imaging Systems and Technology*, 32(5), 1801–1814, 2022.

[17] Chinnam, S.K.R.; Sistla, V., Kolli, V.K.K. (2022). Multimodal attention-gated cascaded U-Net model for automatic brain tumor detection and segmentation, *Biomedical Signal Processing and Control*, 78, 103907, 2022.

[18] Ilhan, A.; Sekeroglu, B., Abiyev, R. (2022). Brain tumor segmentation in MRI images using non-parametric localization and enhancement methods with U-net, *International Journal of computer-assisted radiology and Surgery*, 17(3), 589–600, 2022.

[19] Li, S.; Liu, J., Song, Z. (2022). Brain tumor segmentation based on region of interest-aided localization and segmentation U-Net, *International Journal of Machine Learning and Cybernetics*, 13(9), 2435–2445, 2022.

[20] Mridha, K.; Simanta, S., Limbu, M. (2022). U-Net for Medical Imaging: A Novel Approach for Brain Tumor Segmentation, *Global Journal of Innovation and Emerging Technology*, 1(1), 20–28, 2022.

[21] Chattopadhyay, A.; Maitra, M. (2022). MRI-based brain tumor image detection using CNN-based deep learning method, *Neuroscience informatics*, 2(4), 100060, 2022.

[22] Gan, X.; Wang, L., Chen, Q., Ge, Y., Duan, S. (2021) GAU-Net: U-Net based on global attention mechanism for brain tumor segmentation, In *Journal of Physics: Conference Series*, 1861(1), 012041, 2021. IOP Publishing. DOI 10.1088/1742-6596/1861/1/012041.

[23] Siddique, N.; Paheding, S., Elkin, C.P., Devabhaktuni, V. (2021). U-Net and Its Variants for Medical Image Segmentation: A Review of Theory and Applications, in *IEEE Access*, 9, 82031–82057, 2021, doi: 10.1109/ACCESS.2021.3086020.

[24] Tarkhan, A.; Simon, N., Bengtsson, T., Nguyen, K., Dai, J. (2021). Survival Prediction Using Deep Learning, In *Proceedings of AAAI Spring Symposium on Survival Prediction - Algorithms, Challenges, and Applications*, 2021, in *Proceedings of Machine Learning Research*, 146, 207-214, 2021, Available from https://proceedings.mlr.press/v146/tarkhan21a.html.

[25] Futrega, M.; Milesi, A., Marcinkiewicz, M., Ribalta, P. (2021). Optimized U-Net for brain tumor segmentation, In *International MICCAI Brainlesion Workshop*, Cham: Springer International Publishing, 15–29, 2021.

[26] Maqsood, S.; Damasevicius, R., Shah, F.M. (2021). An efficient approach for the detection of brain tumor using fuzzy logic and U-NET CNN classification, In *Computational Science and Its Applications - ICCSA 2021: 21st International Conference*, Cagliari, Italy, September 13–16, 2021, Proceedings, Part V, Springer International Publishing, 21, 105–118, 2021.

[27] Jwaid, W.M.; Matar Al-Husseini, Z.S., Sabry, A.H. (2021). Development of Brain Tumor Segmentation of Magnetic Resonance Imaging (MRI) using U-Net Deep Learning, *Eastern-European Journal of Enterprise Technologies*, 112, 2021.

[28] Trivedi, H.; Thumar, K., Ghelani, K., Gandhi, D. (2021). An Analysis of Brain Tumor Segmentation Using Modified U-Net Architecture, In *Innovations in Information and Communication Technologies (IICT-2020), Proceedings of International Conference on ICRIHE-2020, Delhi, India: IICT-2020*, Springer International Publishing, 141–147, 2021.

[29] Andreas S. Panayides et al. (2020). AI in Medical Imaging Informatics: Current Challenges and Future Directions, in *IEEE Journal of Biomedical and Health Informatics*, 24(7), 1837–1857, 2020. doi: 10.1109/JBHI.2020.2991043.

[30] Rehman, M.U.; Cho, S. Kim, J.H. Chong, K.T. (2020). BU-Net: Brain Tumor Segmentation Using Modified U-Net Architecture, *Electronics*, 9, 2203, 2020. https://doi.org/10.3390/electronics9122203.

[31] Sunita M. Kulkarni; Sundari, G. (2020). A Framework for Brain Tumor Segmentation and Classification using Deep Learning Algorithm, *International Journal of Advanced Computer Science and Applications (IJACSA)*, 11(8), 2020. http://dx.doi.org/10.14569/IJACSA.2020.0110848.

[32] Eric Ke Wang; Chien-Ming Chen, Mohammad Mehedi Hassan, Ahmad Almogren. (2020). A deep-learning based medical image segmentation technique in Internet-of-Medical-Things domain, *Future Generation Computer Systems*, 108, 135–144, 2020. ISSN 0167-739X, https://doi.org/10.1016/j.future.2020.02.054.

[33] Hazra, D.; Byun, Y. (2020). Brain tumor detection using skull stripping and U-net architecture, *International Journal of Machine Learning and Computing*, 10(2), 400–405, 2020.

[34] Ahmed, S.F., Rahman, F.S., Tabassum, T., Bhuiyan, M.T.I. (2019). 3D U-Net: fully convolutional neural network for automatic brain tumor segmentation, In *2019 22nd International Conference on Computer and Information Technology (ICCIT), IEEE*, 1–6, 2019.

[35] Agrawal Ritu; Sharma Manisha, Singh Bikesh Kumar. (2019). Segmentation of Brain Tumour Based on Clustering Technique: Performance Analysis, *Journal of Intelligent Systems*, 28(2), 291–306, 2019. https://doi.org/10.1515/jisys-2017-0027.

[36] Kermi, A.; Mahmoudi, I., Khadir, M.T. (2019). Deep convolutional neural networks using U-Net for automatic brain tumor segmentation in multimodal MRI volumes, In *Brainlesion: Glioma, Multiple Sclerosis, Stroke, and Traumatic Brain Injuries: 4th International Workshop, BrainLes* 2018, Held in Conjunction with MICCAI 2018, Granada, Spain, September 16, 2018, Revised Selected Papers, Part II 4 (pp. 37-48). Springer International Publishing, 2019.

[37] Zhou, Z.; Siddiquee, M.M.R., Tajbakhsh, N., Liang, J. (2019). Unet++: Redesigning skip connections to exploit multiscale features in image segmentation, *IEEE Transactions on medical imaging*, 39(6), 1856–1867, 2019.

[38] Bahadure, N.B.; Ray, A.K., Thethi, H.P. (2018). Comparative Approach of MRI-Based Brain Tumor Segmentation and Classification Using Genetic Algorithm, *J Digit Imaging*, 477–489, 2018. doi 10.1007/s10278-018-0050-6. PMID: 29344753; PMCID: PMC6113145.

[39] Mehta, R., Arbel, T. (2018). 3D U-Net for brain tumor segmentation, In *Brainlesion: Glioma, Multiple Sclerosis, Stroke, and Traumatic Brain Injuries: 4th International Workshop, BrainLes 2018, Held in Conjunction with MICCAI 2018, Granada, Spain, September 16, 2018, Revised Selected Papers, Part II 4, 254–266. Springer International Publishing*, 2018.

[40] Dong, H.; Yang, G., Liu, F., Mo, Y., Guo, Y. (2017). Automatic Brain Tumor Detection and Segmentation Using U-Net Based Fully Convolutional Networks, In: *Valdés Hernández, M., González-Castro, V. (eds) Medical Image Understanding and Analysis. MIUA 2017. Communications in Computer and Information Science*, Springer, Cham, 723, 2017. https://doi.org/10.1007/978-3-319-60964-5_44.

[41] Pereira, S.; Pinto, A., Alves, V., Silva, C.A. (2016). Brain Tumor Segmentation Using Convolutional Neural Networks in MRI Images, in *IEEE Transactions on Medical Imaging*, 35(5), 1240–1251, 2016. doi: 10.1109/TMI.2016.2538465.

[42] Işın, A.; Direkoğlu, C., Şah, M. (2016). Review of MRI-based brain tumor image segmentation using deep learning methods, *Procedia Computer Science*, 102, 317–324, 2016.

[43] Pan, M.S.; Tang, J.T., Yang, X.L. (2010). A modified adaptive median filter method and its applications in medical images, *Biomedical Engineering: Applications, Basis and Communications*, 22(06), 489–496, 2010.

Copyright ©2024 by the authors. Licensee Agora University, Oradea, Romania.
This is an open access article distributed under the terms and conditions of the Creative Commons Attribution-NonCommercial 4.0 International License.
Journal's webpage: http://univagora.ro/jour/index.php/ijccc/

C O P E
Member since 2012
JM08090

This journal is a member of, and subscribes to the principles of,
the Committee on Publication Ethics (COPE).
https://publicationethics.org/members/international-journal-computers-communications-and-control

Cite this paper as:

Pearline Sheba Grace, J.; Ezhilarasi. P., Rajesh Kannan, S. (2024), Unveiling the Secrets of Brain Tumors: A Fuzzy C-Means and U-Net Convolution Approach for Enhanced Segmentation, *International Journal of Computers Communications & Control*, 19(2), 5732, 2024.
https://doi.org/10.15837/ijccc.2024.2.5732